Fitoterapia 139 (2019) 104377

Contents lists available at ScienceDirect

Fitoterapia

journal homepage: www.elsevier.com/locate/fitote

Montbresides A–D: antibacterial *p*-coumaroyl esters of a new sucrose-based tetrasaccharide from *Crocosmia* × *crocosmiiflora* (montbretia) flowers

Shagufta Perveen[a,*], Ian H. Sadler[b], Raha Orfali[a], Areej Mohammad Al-Taweel[a], Lorna Murray[b], Stephen C. Fry[c,*]

[a] Department of Pharmacognosy, College of Pharmacy, King Saud University, Riyadh, Saudi Arabia,
[b] School of Chemistry, The University of Edinburgh, UK
[c] The Edinburgh Cell Wall Group, Institute of Molecular Plant Sciences, The University of Edinburgh, UK

ARTICLE INFO

Keywords:
Crocosmia × *crocosmiiflora*
Phenolic glycoside
Sucrose-based tetrasaccharide
Montbresides A–D
Cytotoxicity
Antibacterial activity

ABSTRACT

Crocosmia × *crocosmiiflora* (montbretia) flowers yielded four esters (montbresides A–D) of a new sucrose-based tetrasaccharide, 3-*O*-β-D-glucopyranosyl-4′-*O*-α-D-rhamnopyranosyl-sucrose [β-D-Glc-(1 → 3)-α-D-Glc-(1↔2)-β-D-Fru-(4 ← 1)-α-D-Rha]. All four possess *O*-*p*-coumaroyl residues on C-3 of fructose and C-4 of α-glucose, plus *O*-acetyl residues on C-2 and C-3 of rhamnose and C-6 of fructose. Montbresides A and B are additionally *O*-acetylated on C-1 of fructose. The *p*-coumaroyls are *trans*- in montbresides A and C and *cis*- in B and D. Elemental compositions were determined from MS data, and structures from 1D and 2D NMR spectra. Monosaccharide residues were identified from selective 1D TOCSY spectra and TLC, and acylation sites from 2D HMBC spectra. Enantiomers were distinguished by enzymic digestion. Montbretia flower extracts were cytotoxic against six human cancerous cell-lines, but purified montbresides lacked cytotoxicity. Each montbreside displayed antibacterial activity against *Staphylococcus aureus* (minimal inhibitory concentration ~6 μg/ml). Montbretia is a potential source of new cytotoxins and antibacterial agents.

1. Introduction

Crocosmia × *crocosmiiflora* (Lemoine) N.E. Br. (montbretia; family Iridaceae, order Asparagales; a monocotyledon) is a popular garden plant with striking orange flowers in late summer, and is used as an antitumour agent in Japanese folk medicine. Hot-water extracts of its corms show antitumour activity, the active principle being a mixture of saponins [1]. Montbretia extracts also have antioxidant activity [2]. Saponins and flavonoid glycosides are major secondary metabolites of this plant [3]. In the present work, we found that butanolic extracts of montbretia flowers are cytotoxic against six human cancer cell-lines. These extracts contained three known secondary metabolites and four new phenol–sugar conjugates, characterised here chemically (Fig. 1) and in terms of their cytotoxic and antibacterial properties.

2. Experimental

2.1. General experimental procedures

Proton 1D NMR spectra, selective 1D proton TOCSY and proton ROESY experiments were recorded at 800 MHz on a Bruker AVANCE III instrument. Carbon-13 1D NMR spectra, proton 2D-COSY spectra, a proton NOESY spectrum and 1-bond carbon–proton chemical shift correlation (HSQC) spectra were recorded on a Bruker AMX-500 instrument (125 MHz for ^{13}C). Multiple bond carbon–proton chemical shift correlation (HMBC) spectra were recorded for montbresides A–C on a Bruker AMX-500 instrument and for montbreside D on a Bruker AV-700 instrument (175 MHz for ^{13}C). Proton spectra were referenced to the residual $CD_2\underline{H}OD$ signal at 3.33 ppm. Carbon spectra were referenced to $\underline{C}D_3OD$ at 49.0 ppm. Chemical shifts are given in ppm (δ) relative to tetramethylsilane, and scalar coupling constants (*J*) are given in Hz. For montbresides A and C, selective 1D TOCSY experiments were carried out in which the mixing times were successively increased from 20 to 160 ms for each of the resonances chosen for initiating the magnetisation transfer.

Exact mass measurements were made on a Bruker 'micrOTOF II' instrument with ES ionization, in positive ion mode.

Montbresides were alkali-hydrolysed in NaOH (routinely 8 mM) at 25 °C for 18 h, then acidified with HOAc and analysed by TLC. Mild and complete acid hydrolysis of the tetrasaccharide were performed in 80 mM trifluoroacetic acid (TFA) at 70 °C (routinely 9 h), and 2 M TFA at 120 °C (1 h) respectively. TFA was removed in a 'SpeedVac' at 25 °C,

* Corresponding authors at: The University of Edinburgh, UK and King Saud University, Saudi Arabia.
E-mail addresses: shagufta792000@yahoo.com (S. Perveen), s.fry@ed.ac.uk (S.C. Fry).

https://doi.org/10.1016/j.fitote.2019.104377
Received 16 September 2019; Received in revised form 13 October 2019; Accepted 18 October 2019
Available online 19 October 2019
0367-326X/

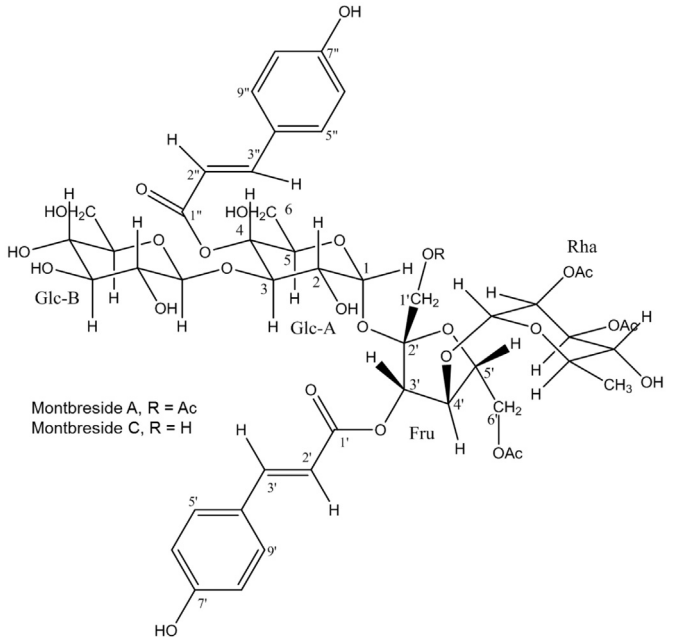

Fig. 1. Montbresides A and C. Montbresides B and D are identical to these but the coumarate residues are in the *cis*-configuration.

and products were analysed by TLC. Enzymic digestion of the tetrasaccharide was performed with a 1% (*w/v*) solution of Driselase (Sigma–Aldrich; purified as in [4]) in pyridine/HOAc/H_2O (1:1:98, containing 0.5% chlorobutanol) at 25 °C for 0–99 h; products were analysed by TLC on Merck silica-gel plates in butan-1-ol/acetic acid/water (4:1:1) or ethyl acetate/pyridine/acetic acid/water (6:3:1:1) with 1–3 ascents. Staining was with iodine vapour or thymol/H_2SO_4 [5].

2.2. Plant material

Montbretia [*Crocosmia* × *crocosmiiflora* (Lemoine) N.E. Br. (monocot: Asparagales: Iridaceae)] flowers (500 g) were collected from gardens in Edinburgh, in July 2017, and identified by SCF. Voucher specimen: Royal Botanic Garden Edinburgh, herbarium barcode E00873192.

2.3. Extraction and isolation

Montbretia flowers (collected in July 2017) were air-dried (40 g dry weight), powdered, stored dry at room temperature in the dark, and percolated with 2 × 1.5 l of 80% (*v*/v) ethanol at 25 °C in the dark (August 2017). The extract was concentrated in vacuo to a residue (15 g), which was stored dry at room temperature in the dark then suspended in water (150 ml; September 2017) and partitioned against first chloroform (2.0 l) then butan-1-ol (2.5 l). The butanol fraction was dried (8 g), redissolved in 25 ml water and passed through Sephadex LH-20 (3 × 70 cm) with a 0 → 100% methanol gradient (4 l total) to afford five fractions (A–E; September 2017), which were monitored by TLC on silica-gel and RP-18 F_{254} (Merck, Darmstadt, Germany) in methanol/water/acetic acid (10:10:1; detection was under 254-nm UV and by spraying with $Ce(SO_4)_2$ followed by heating at 150 °C which blackened the UV spots. The fractions were stored as solutions at 5 °C in the dark. The chloroform and aqueous fractions and the butanolic fractions A and B, which between them are expected to contain most of the quantitatively major phytochemicals such as sucrose, glucose, fructose, citrate, malate, glutamate etc., did not show up under UV and were not characterised further.

Fraction C (1 g), which eluted from Sephadex LH-20 in 20% methanol, was further resolved by silica-gel (Merck) column chromatography (1 × 100 cm) with $CHCl_3$/methanol (9:1 → 6:4, *v*/v; total 1 l) and fractions were monitored by TLC ($CHCl_3$/methanol, 3:1) to afford two major sub-fractions C1 and C2 (October 2017), which were then stored as solutions at 5 °C in the dark. Sub-fraction C1 (150 mg) was re-run (November 2017) on the same silica-gel column with $CHCl_3$/methanol (8:2, *v*/v) to afford montbresides C (15 mg) and D (16 mg). Sub-fraction C2 (250 mg) was also re-run (December 2017) on the same silica gel column, eluting with $CHCl_3$/methanol (9:1 → 7:3, *v*/v) to yield montbresides A (15 mg) and B (19 mg). Fraction D (0.5 g), which eluted in 30% methanol, was re-run (December 2017) on the silica gel column in $CHCl_3$/methanol (4:1, v/v), yielding cinnamic acid glucosyl ester (**5**; 28 mg). Fraction E (500 mg), which eluted in 40% methanol, was sub-fractionated by HPLC (on ODS gel (Inertsil ODS-3, GL-science, 10 × 250 mm) in 50% methanol at 1.0 ml/min; January 2018), to afford *trans-p*-coumaric acid (**6**; 18 mg) and *trans*-cinnamic acid (**7**; 25 mg).

2.4. Spectroscopic data of compounds

Selected NMR and mass spectra of montbresides A–D are in the supplementary data.

Montbreside A: White amorphous powder; $[\alpha]_{25}D$ + 37 (c 0.0010, methanol); ^1H NMR (800 MHz, methanol-d_4) data, see Table 1; ^{13}C NMR (125 MHz, methanol-d_4) data, see Table 2; HRESIMS *m/z* 1133.3297 $[M.Na]^+$ (calcd for $C_{50}H_{62}O_{28}$·Na, 1133.33198).

Montbreside B: White amorphous powder; $[\alpha]_{25}D$ + 48 (c 0.0015, methanol); NMR as above; HRESIMS *m/z* 1133.3299 $[M.Na]^+$ (calcd for $C_{50}H_{62}O_{28}$·Na, 1133.33198).

Montbreside C: White amorphous powder; $[\alpha]_{25}D$ + 44 (c 0.0012, methanol); NMR as above; HRESIMS *m/z* 1091.3209 $[M.Na]^+$ (calcd for $C_{48}H_{60}O_{27}$·Na, 1091.3214).

Montbreside D: White amorphous powder; $[\alpha]_{25}D$ + 52 (c 0.0012, methanol); NMR as above; HRESIMS *m/z* 1091.3210 $[M.Na]^+$ (calcd for $C_{48}H_{60}O_{27}$·Na, 1091.3214).

2.5. Cytotoxicity assay

MCF-7 cells (human breast cancer cell line), HCT-116 (colon carcinoma), HepG-2 cells (human hepatocellular carcinoma), HeLa (cervical carcinoma), A-549 (lung carcinoma) and WI-38 (human lung fibroblast normal cells) were obtained from Vacsera (Giza, Egypt). The cells were cultured in Dulbecco's modified Eagle's medium with 10% heat-inactivated foetal bovine serum, HEPES buffer (0.1 M, pH 7.0), 1% L-glutamine and 50 µg/ml gentamycin. The cells were kept at 35 °C under humidified condition with 5% CO_2 and were sub-cultured twice a week. Montbresides (up to 50 µg/ml) were evaluated for cytotoxicity against these six cell-lines by the MTT method (reduction of a tetrazolium dye [6]).

2.6. Antibacterial assay

Antibacterial activities were assayed by the methods of [7]. Pathogenic bacteria, including Gram-negatives [*Pseudomonas aeruginosa* (NR-117678.1), *Escherichia fergusonii* (CU928158.2), *Enterobacter xiangfangensis* (CP017183.1)] and Gram-positives [*Bacillus licheniformis* (KX785171.1), *Staphylococcus aureus* (CP011526.1)] were suspended for 24 h in nutrient broth. After spreading on Müller–Hinton agar plates, wells were filled with 10 µl of various concentrations of each sample (up to 25 µg/ml). Amikacin was the positive control. The diameters of clear (inhibited) zones were measured. The experiment was conducted three times; the mean value of minimal inhibitory concentration (MIC [8]) is reported.

Table 1
^{1}H NMR spectroscopic data (800 MHz) for montbresides A–D.

Position	δ (ppm) of montbreside				Multiplicity[a]		*J* (Hz) of montbreside			
	A	B	C	D			A	B	C	D
Fru-1a	4.220	4.209	3.649	3.634	d	*J* 1a 1b	12.0	12.0	12.4	12.3
Fru-1b	4.286	4.331	3.737	3.732	d					
Fru-3	5.635	5.588	5.680	5.642	d	*J* 3 4	7.4	7.5	6.7	7.1
Fru-4	4.689	4.579	4.627	4.530	dd	*J* 4 5	7.4	7.5	6.7	7.1
Fru-5	4.295	4.261	4.626	4.266	ddd	*J* 5 6a	5.6	5.4	5.8	5.7
Fru-6a	4.412	4.354	4.424	4.344	dd	*J* 5 6b	6.1	6.2	6.2	6.1
Fru-6b	4.493	4.452	4.468	4.429	dd	*J* 6a 6b	11.7	11.7	11.6	11.7
Cou-2′	6.482	5.909	6.479	5.908	d	*J* 2 3	15.9	12.7	15.9	12.8
Cou-3′	7.828	7.015	7.813	6.992	d					
Cou-5′, 9′	7.570	7.734	7.570	7.752	so	*J* 5 6	8.7	8.7	8.7	8.8
Cou-6′, 8′	6.793	6.812	6.794	6.803	so					
Glc-A-1	5.503	5.473	5.511	5.478	d	*J* 1 2	3.8	3.6	3.7	3.8
Glc-A-2	3.723	3.739	3.757	3.743	dd	*J* 2 3	9.7	9.6	9.4	9.4
Glc-A-3	3.986	3.939	4.001	3.960	t	*J* 3 4	9.4	9.5	9.4	9.4
Glc-A-4	4.996	4.992	5.007	4.996	dd	*J* 4 5	10.0	10.0	10.2	10.2
Glc-A-5	4.286	4.113	4.276	4.124	ddd	*J* 5 6a	5.2	4.5	5.0	4.5
Glc-A-6a	3.617	3.576	3.605	3.733	dd	*J* 5 6b	2.3	2.2	2.2	2.3
Glc-A-6b	3.766	3.733	3.765	3.579	dd	*J* 6a 6b	12.3	12.4	12.4	12.3
Cou-2″	6.172	5.869	6.141	5.866	d	*J* 2 3	15.9	12.7	15.9	12.8
Cou-3″	7.598	6.910	7.590	6.909	d					
Cou-5″, 9″	7.378	7.689	7.368	7.693	so	*J* 5 6	8.7	8.7	8.7	8.8
Cou-6″, 8″	6.845	6.780	6.846	6.781	so					
Glc-B-1	4.320	4.373	4.338	4.363	d	*J* 1 2	7.8	7.8	7.8	7.8
Glc-B-2	3.118	3.158	3.128	3.164	dd	*J* 2 3	9.2	9.2	9.3	9.3
Glc-B-3	3.230	3.240	3.243	3.254	t	*J* 3 4	9.2	9.2	9.0	9.1
Glc-B-4	3.258	3.182	3.262	3.189	t	*J* 4 5	9.2	9.2	9.2	9.7
Glc-B-5	2.895	3.037	2.940	3.037	ddd	*J* 5 6a	4.0	5.2	4.1	5.1
Glc-B-6a	3.410	3.546	3.431	3.547	dd	*J* 5 6b	2.5	2.7	2.6	2.8
Glc-B-6b	3.484	3.692	3.507	3.687	dd	*J* 6a 6b	11.7	11.6	11.7	11.6
Rha-1	4.953	4.906	4.941	4.897	d	*J* 1 2	1.8	1.9	1.8	1.9
Rha-2	5.237	5.223	5.229	5.216	dd	*J* 2 3	3.3	3.5	3.4	3.4
Rha-3	5.034	5.031	5.036	5.032	dd	*J* 3 4	9.9	10.0	9.9	9.9
Rha-4	3.499	3.507	3.499	3.499	t	*J* 4 5	9.9	9.6	9.6	9.9
Rha-5	3.792	3.796	3.816	3.820	dq	*J* 5 6	6.2	6.2	6.1	6.2
Rha-6	1.255	1.256	1.260	1.257	d					
CH_3	2.018	2.020	2.018	2.018	s					
CH_3	2.094	2.105	2.095	2.093	s					
CH_3	2.118	2.114	1.108	2.112	s					
CH_3	2.159	2.142			s					

[a] so = second order spectrum (couplings approximate), s = singlet, d = doublet, t = triplet, q = quartet; Cou = *p*-coumaroyl.

3. Results and discussion

3.1. Source of four new glycol-conjugates

The crude ethanolic extract of montbretia flowers showed moderate cytotoxicity on five of six tested human cancer cell lines; a butanol-partitioning sub-fraction showed enhanced cytotoxicity on all six lines (Table 3). We therefore examined the butanol sub-fraction for secondary metabolites. HPLC revealed at least 7 UV-absorbing phytochemicals (Fig. S1): four new compounds [montbresides A–D] and three known compounds (*p*-coumaric acid, *trans*-cinnamic acid and *trans*-cinnamoyl β-glucosyl ester). The four montbresides were isolated by open-column chromatography and their elemental compositions determined by ESI-MS (Fig. S2). As described below their structures were elucidated from their 1D and 2D NMR spectra (Figs. S3–S14) and by TLC of their hydrolysis products (Fig. 3 and Figs. S15–S17).

3.2. Structure of montbreside A

Montbreside A ($C_{50}H_{62}O_{28}$) was shown to be 3-*O*-β-D-glucopyranosyl-3′,4-di-*O*-*trans*-*p*-coumaroyl-4′-*O*-(2,3-di-*O*-acetyl-α-D-rhamnopyranosyl)-1′,6′-di-*O*-acetylsucrose as follows. Its ^{1}H (Table 1) and ^{13}C (Table 2) spectra showed the presence of two *trans*-coumaroyl groups ($J_{2'\text{-}3'} = J_{2''\text{-}3''} = 15.9$ Hz) and four acetyl groups. The signals corresponding to the two coumaroyl groups were distinguished and assigned from the 2D HSQC (proton–carbon one-bond correlation) spectrum (Fig. S12) and the 2D HMBC (proton–carbon multiple bond correlation) spectrum (Figs. S13 and S18). The carbonyl signals of the acetyl groups (δ 171.8, 172.3 × 2, 172.7) were identified by their ^3J correlations to the methyl proton signals (δ 2.02, 2.09, 2.12, 2.16). In addition to the signals from these groups, the 1D single-pulse and DEPT ^{13}C spectra show one methyl group, four oxygen-bearing CH_2 groups, eighteen oxygen-bearing CH groups, and an oxygen-bearing quaternary carbon. This suggested the presence of a tetrasaccharide composed of four hexoses. The position of the methyl doublet protons suggested the presence of either a rhamnose or a fucose residue and the position of the quaternary carbon suggested the presence of a ketose, possibly fructose. Although at 800 MHz the proton spectrum shows some signal overlap in the δ 3.0–6.0 ppm region, careful analysis of the COSY spectrum (Figs. S6 and S7) and of a series of selective 1-D TOCSY spectra (Fig. 2), where clearly separated signals were used to initiate the magnetisation transfer, allowed the identification of two glucpyranose residues (Glc-A and Glc-B), a rhamnopyranose residue (Rha) and a fructofuranose residue (Fru) [pyranose and furanose not stated hereafter].

These spectra also allowed the assignment of their individual proton signals (Table 1). The HSQC spectrum allowed the assignment of the corresponding ^{13}C signals (Table 2). The anomeric protons' H1–H2 coupling constants in the glucose residues showed that Glc-A has H-1 equatorial (δ 5.50 d, 3.8 Hz) whereas Glc-B has it axial (δ 4.32 d, 7.8 Hz); thus Glc-A and Glc-B are α- and β-linked respectively.

Table 2
^{13}C NMR spectroscopic data (125 MHz) for montbresides A–D.

Position	δ (ppm) of montbreside			
	A	B	C	D
Fru-1	64.8	66	64.8	65.0
Fru-2	102.9	104.2	106.1	105.9
Fru-3	76.7	77.8	78.0	77.8
Fru-4	80.9	82.4	82.9	82.3
Fru-5	78.5	79.7	80.0	79.9
Fru-6	64.1	65.4	65.4	65.6
Cou-1′	167.8	167.0	167.7	166.9
Cou-2′	114.2	115.3	114.4	115.8
Cou-3′	148.1	146.9	147.9	146.5
Cou-4′	126.9	127.3	126.8	127.5
Cou-5′ & 9′	131.5	134.1	131.4	134.2
Cou-6′ & 8′	117.2	116.1	117.1	116.1
Cou-7′	161.6	160.3	161.5	160.3
Glc-A-1	93.0	93.2	92.7	92.9
Glc-A-2	72.3	72.5	72.6	73.0
Glc-A-3	82.8	82.0	83.1	83.2
Glc-A-4	70.8	69.9	70.6	69.9
Glc-A-5	72.5	72.4	72.4	72.4
Glc-A-6	62.0	61.8	61.8	61.8
Cou-1″	168.5	167.3	168.6	167.3
Cou-2″	114.8	116.6	114.7	116.7
Cou-3″	147.2	145.6	147.3	145.5
Cou-4″	126.9	127.4	126.9	127.5
Cou-5″ & 9″	131.3	133.8	131.4	133.9
Cou-6″ & 8″	117.0	115.9	117.0	115.9
Cou-7″	161.2	160.0	161.2	160.2
Glc-B-1	106.1	105.4	106.0	105.5
Glc-B-2	75.8	75.7	75.8	75.8
Glc-B-3	77.4	77.6	77.3	77.7
Glc-B-4	70.5	71.4	70.6	71.4
Glc-B-5	77.3	77.5	77.3	77.6
Glc-B-6	61.8	62.8	61.8	62.8
Rha-1	99.4	99.5	99.3	99.5
Rha-2	70.9	71.0	71.0	71.1
Rha-3	72.7	72.8	72.7	72.8
Rha-4	71.0	71.1	71.0	71.2
Rha-5	70.8	70.8	70.8	70.9
Rha-6	18.0	18.0	18.1	18.0
C=O	171.8	171.8	171.9	171.8
C=O	172.3	172.3	172.4	172.2
C=O	172.3	172.3	–	–
C=O	172.7	172.7	172.8	172.7
CH_3	20.7	20.7	20.7	20.7
CH_3	20.8	20.8	20.8	20.8
CH_3	20.8	20.8	20.9	20.8
CH_3	20.9	20.9	–	–

The linkages between the monosaccharide residues were deduced from the HMBC spectrum (Fig. S13 and S18):

1. Correlation of Fru-C2 (δ 102.9) with Glc-A-H1 (δ 5.50) shows that Glc-A-C1 is *O*-linked to Fru-C2 as in sucrose. Fru-C2 (δ 102.9) also shows a correlation with Fru-H1 (δ 4.22, 4.29), supporting the assignment of Fru-C2.
2. Correlation of Fru-C4 (δ 80.9) with Rha-H1 (δ 4.95), and of Rha-C1 (δ 99.4) with Fru-H4 (δ 4.69) showed that Rha-C1 is *O*-linked to Fru-C4. The 2D NOESY and ROESY spectra showed strong correlations between the axial protons of Rha-H3 (δ 5.03) and Rha-H5 (δ 3.79) but no correlation of either with Rha-H1 (δ 4.95), suggesting that Rha-H1 is equatorial and therefore Rha is α-linked to Fru [9].
3. Correlation of Glc-A-C3 (δ 82.8) with Glc-B-H1 (δ 4.32) and of Glc-B-C1 (δ 106.1) with Glc-A-H3 (δ 3.99) showed that Glc-B-C1 is *O*-linked (β) to Glc-A-C3 (i.e. as in laminaribiose). These linkages were supported by correlations between Glc-A-H3 and Glc-B-H1 and between Rha-H1 and Fru-H4 in the 2D NOESY spectrum (Fig. S10).

The sites to which the four acetyl groups and the two coumaroyl groups are linked were also deduced from the HMBC spectrum. Correlations of Rha-H2 (δ 5.24), Rha-H3 (δ 5.03), Fru-H1 (δ 4.22, 4.29) and Fru-H6 (δ 4.41, 4.49) to acetyl carbonyl signals (δ 171.8, 172.3 × 2, 172.7) showed that the the *O*-acetyl groups were linked to Rha-C2, Rha-C3, Fru-C1 and Fru-C6. Furthermore, Fru-H3 (δ 5.64) and Glc-A-H4 (δ 5.00) show long-range correlations to the carbonyl signals of coumaroyl groups A (δ 167.8) and B (δ 168.5) respectively, showing that the *O*-coumaroyl groups are linked to Fru-C3 and Glc-A-C4 [9].

To support the proposed structure of the oligosaccharide core of montbreside A, we removed all acyl residues by mild alkaline hydrolysis, yielding an alkali-stable (thus non-reducing) tetrasaccharide plus coumaric acid (Fig. S15). On complete acid hydrolysis, the tetrasaccharide gave glucose and rhamnose (Fig. S16; any fructose would have been degraded under these conditions), confirming that the deoxysugar is rhamnose not fucose. The de-acylated tetrasaccharide was also partially hydrolysed with mild acid, which specifically targets furanosyl linkages. Under conditions optimised on pure sucrose (80 mM TFA, 70 °C, 0–9 h), the tetrasaccharide was gradually hydrolysed into two disaccharides, **D1** and **D2** (Fig. S17). **D1** co-migrated with laminaribiose [β-D-Glc*p*-(1 → 3)-D-Glc] in two TLC systems (Fig. S16), supporting the NMR data. **D2** had a higher R_F and did not co-migrate with any standard disaccharide available (Fig. S16). As the presence of a fructose residue is demonstrated by the NMR results, we propose that **D2** is α-D-Rha*p*-(1 → 4)-D-Fru. The failure of mild acid to release Glc and Rha as monomers confirms that the β-D-Glc and α-D-Rha residues are pyranose.

To further explore the anomerism and enantiomerism of the tetrasaccharide's monosaccharide residues, we digested it with 'Driselase', a commercial mixture of fungal enzymes which does not hydrolyse sucrose (Fig. 3) but which possesses β-D-glucosidase and α-L-rhamnosidase activities [4]. As expected, a single glucose was released leaving a stable trisaccharide, proposed to be rhamnopyranosyl sucrose (Fig. 3). Since Driselase did not release rhamnose from the tetrasaccharide it cannot be present as α-L-rhamnose. Thus, since the NMR data show its H1 is equatorial, it must be α-D-rhamnose.

Table 3
Cytotoxicity of montbretia flower extract and four purified montbresides on six human cancer cell-lines.

Sample	IC50[a] (μg/ml ± SD; *n* = 3) of sample on cell-line					
	MCF-7	HCT-116	HepG-2	HeLa	A-549	WI-38
Crude ethanolic extract	45.0 ± 9.3	37.8 ± 26.9	46.9 ± 42.7	41.2 ± 3.6	39.1 ± 15.3	> 50
Butanol-partitioning sub-fraction	22.8 ± 1.7	12.5 ± 0.5	11.5 ± 0.4	18.3 ± 3.9	9.6 ± 1.7	38.6 ± 4.6
Montbreside A	> 50	> 50	> 50	> 50	> 50	> 50
Montbreside B	> 50	> 50	> 50	> 50	> 50	> 50
Montbreside C	> 50	> 50	> 50	> 50	> 50	> 50
Montbreside D	> 50	> 50	> 50	> 50	> 50	> 50
Vinblastine sulphate (control)	5.44 ± 0.57	2.58 ± 0.43	3.48 ± 0.22	6.54 ± 0.39	3.58 ± 0.48	8.58 ± 0.58

[a] Concentration giving 50% loss of viability.

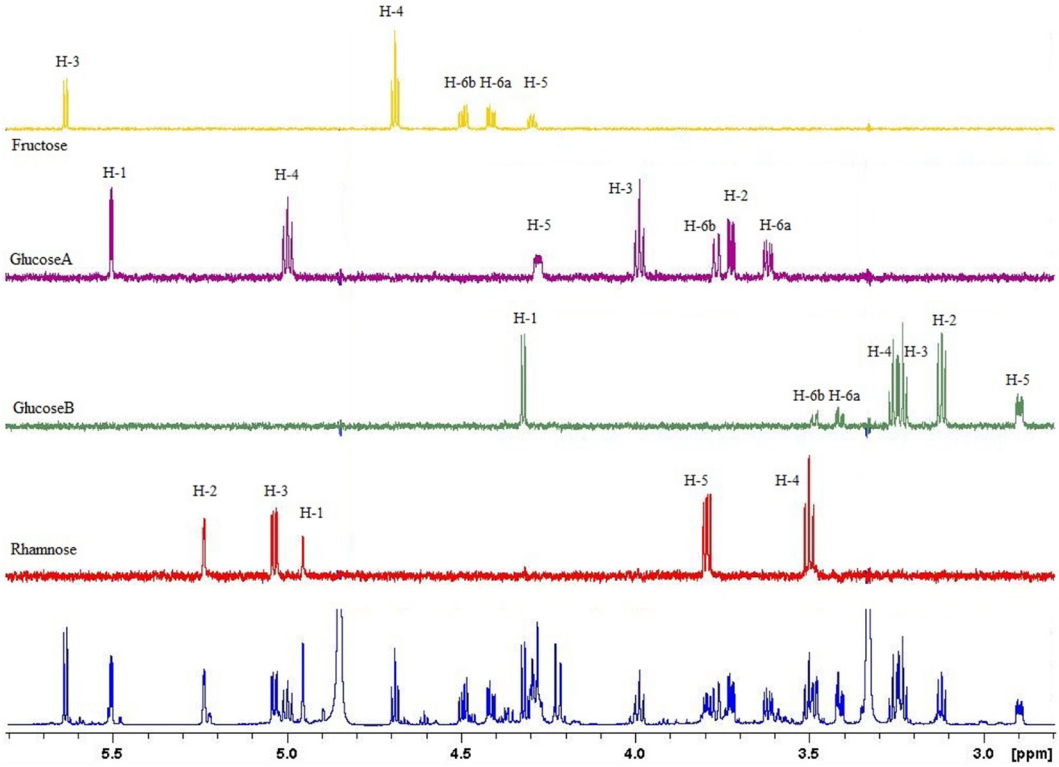

Fig. 2. Region 2.8–5.8 ppm of 800-MHz proton NMR spectrum (lowest trace) of montbreside A and 1D TOCSY spectra showing the separate monosaccharide residues. For the spectra shown, a mixing time of 160 ms was used and magnetization transfer was initiated at H-4 for fructose, glucose A and rhamnose and at H-2 for glucose B.

3.3. Structure of montbreside B

Montbreside B ($C_{50}H_{62}O_{28}$) was structurally elucidated as for A and by comparison of its 1D and 2D NMR spectra with those of A. The only difference between B and A is that the double bonds of the two coumaroyl groups in B have the *cis* configuration ($J_{2'\text{-}3'} = J_{2''\text{-}3''} = 12.7$ Hz) (Table 1). Thus, montbreside B ia 3-*O*-β-D-glucopyranosyl-3′,4-di-*O*-*cis*-*p*-coumaroyl-4′-*O*-(2,3-di-*O*-acetyl-α-D-rhamnopyranosyl)-1′,6′-di-*O*-acetylsucrose.

3.4. Structure of montbreside C

Montbreside C ($C_{48}H_{60}O_{27}$) was treated similarly and the 1D and 2D NMR spectra were compared with those of B and D. The ^{1}H and ^{13}C spectra of C show the presence of only three acetyl groups (δ 171.9, 172.4 & 172.8) and that the coumaroyl groups are trans ($J_{2'\text{-}3'} = J_{2''\text{-}$

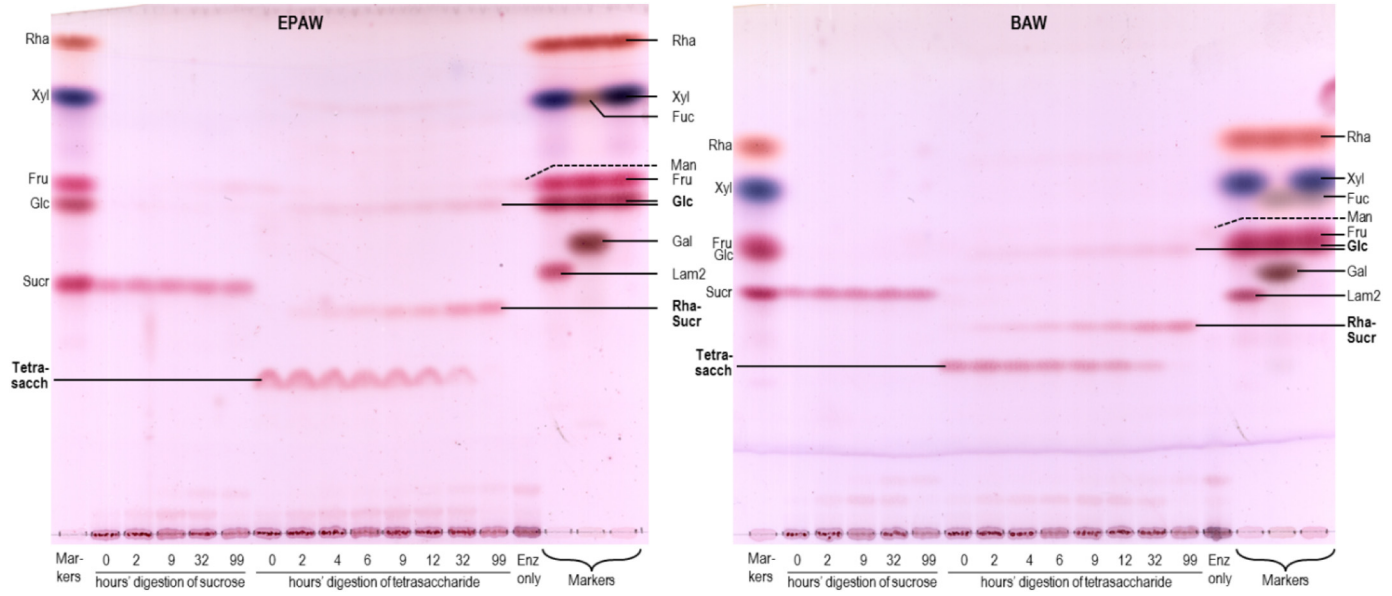

Fig. 3. Driselase digestion of the tetrasaccharide from montbreside A. Driselase (10 mg/ml) was incubated with the tetrasaccharide at 25 °C for 0–99 h. Sucrose was incubated similarly as a control. TLC solvents: EPAW, ethyl acetate/pyridine/HOAc/H_2O 6:3:1:1 (3 ascents); BAW, butan-1-ol/acetic acid/H_2O, 4:1:1 (2 ascents). Lam2, laminaribiose; Rha-Sucr, new trisaccharide product. Mannose (Man) is a trace autolysis product of Driselase.

Table 4
Antimicrobial activities of montbresides and amikacin on five bacterial species.

Compounds	Minimal inhibitory concentration (MIC; μg/ml) against				
	S. aureus	*B. licheniformis*	*E. xiangfangensis*	*E. fergusonii*	*P. aeruginosa*
Montbreside A	6.5	> 25	> 25	18.5	> 25
Montbreside B	6.4	> 25	> 25	17.0	> 25
Montbreside C	5.4	12.0	> 25	> 25	> 25
Montbreside D	5.2	10.5	> 25	> 25	> 25
Amikacin	< 0.52	< 0.52	< 0.52	< 0.52	< 0.52

$_{3''}$ = 15.9 Hz) (Tables 1, 2). The only difference between A and C is that Fru-1 of C bears a hydroxyl group that is not acetylated. Selective 1D-TOCSY experiments allowed the unambiguous assignment of the signals from the protons attached to C6 of the two glucose residues. Thus, montbreside C is 3-*O*-β-D-glucopyranosyl-3′,4-di-*O*-*trans*-*p*-coumaroyl-4′-*O*-(2,3-di-*O*-acetyl-α-D-rhamnopyranosyl)-6′-*O*-acetylsucrose.

3.5. Structure of montbreside D

Montbreside D ($C_{48}H_{60}O_{27}$) was structurally elucidated as for A and by comparison of its 1D and 2D NMR spectra with those of B. The proton spectrum of D shows the presence of only three acetyl groups and that the double bonds of the two coumaroyl groups in **4** have the *cis* configuration ($J_{2'-3'} = J_{2''-3''} = 12.8$ Hz. The only difference between C and D is that the two coumaroyl groups in D are *cis*. The HMBC spectrum showed correlations of only Rha-H2 (δ 5.22), Rha-H3 (δ 5.03), and Fru-H6 (δ 4.34, 4.43) to acetyl carbonyl signals (δ 171.8, 172.2, 172.7) (Tables 1, 2). Thus, montbreside D is 3-*O*-β-D-glucopyranosyl-3′,4-di-*O*-*cis*-*p*-coumaroyl-4′-*O*-(2,3-di-*O*-acetyl-α-D-rhamnopyranosyl)-6′-*O*-acetylsucrose.

For all the montbresides A–D, the signals for Fru-H3, Fru-H5, Fru-H6 and Glc-A-H4 are shifted (δ ~0.5–1.5 ppm) to high frequency than the corresponding signals in sucrose, and the signals for Rha-H2 and Rha-3 are shifted (δ ~1.3 ppm) to high frequency than the corresponding signals in rhamnose. The proton signals for Fru-H1 in A and B lie to high frequency (δ ~0.5 ppm) of those in C and D and the corresponding signals in sucrose. These shifts are consistent with esterification of the hydroxyl groups of sugar moieties.

3.6. Biological activities

Unlike the crude ethanolic extract and the total butanol-partitioning sub-fraction, purified montbresides lacked cytotoxicity against cancer cell-lines (Table 3). However, purified montbresides did exhibit antimicrobial effects on some or all of the bacteria tested (Table 4). *S. aureus* (Gram +ve) was particularly susceptible to all montbresides (MIC ≈ 6 μg/ml). Montbresides A and B inhibited *E. fergusonii* (Gram –ve; MIC ≈ 18 μg/ml) and montbresides C and D inhibited *B. licheniformis* (Gram +ve; MIC ≈ 11 μg/ml). None of the montbresides showed antimicrobial activities against *E. xiangfangensis* and *P. aeruginosa* (both Gram –ve).

3.7. Taxonomic significance

Montbresides are esters of a new sucrose-based tetrasaccharide. Sucrose is a major primary metabolite in plants, and therefore readily available as a foundation for the biosynthesis of glycoconjugates. Nevertheless, sucrose-based secondary metabolites such as those reported are relatively rare; examples include coumaroylated sucrose derivatives [10]. Another highly unusual feature of montbresides is that the rhamnose residue is the D- rather than the common L-enantiomer. The latter is ubiquitous in plants as a component of pectic rhamnogalacturonans [11], and also occurs in a sucrose-based secondary metabolite, 3-*O*-(α-L-rhamnopyranosyl-(1 → 4)-α-L-rhamnopyranosyl)-4,3′-di-*O*-*trans*-*p*-coumaroylsucrose [12]. D-Rhamnose residues are well known in bacterial polysaccharides [13], but in plants they appear to be confined to a small number of secondary metabolites, albeit widely spread taxonomically. For example, α-D-Rha occurs in saponins of onion (monocot, Asparagales) [14] and *Akebia* (dicot, Ranunculales) [15] and an oleanane triterpenoid from *Hibiscus* (dicot, Malvales) [16], and β-D-Rha in arylnaphthalene lignans from *Acanthus* (dicot, Lamiales) [17]. Our report of α-D-Rha in a secondary metabolite is from *Crocosmia* (monocot, Asparagales), confirming the taxonomic breadth of its occurrence.

4. Conclusions

Four new phenolic glyco-conjugates, montbresides A–D, were isolated from montbretia flowers and structurally identified by MS, 1D and 2D NMR spectroscopy, and TLC. The montbresides are of exceptional structural complexity, and their occurrence is taxonomically unique. Unlike crude montbretia flower extracts, purified montbresides lacked cytotoxicity against all tested cancer cell-lines. Thus, the crude extracts can be re-examined for anti-cancer compounds. Purified montbresides did exhibit antimicrobial activities against certain bacterial species.

Funding resources

Supported by a grant from the 'Research Center of the Female Scientific and Medical Colleges', Deanship of Scientific Research, King Saud University and by the UK Biotechnology and Biological Sciences Research Council (BBSRC; grant no. BB/N002458/1).

Declaration of Competing Interest

The authors declare that there is no conflict of interest.

Appendix A. Supplementary data

Supplementary data to this article can be found online at https://doi.org/10.1016/j.fitote.2019.104377.

References

[1] N. Nagamoto, H. Noguchi, A. Itokawa, K. Nakata, K. Namba, H. Nishimura, M. Matsui, M. Mizuno, Antitumor constituents from bulbs of *Crocosmia crocosmiiflora*, Planta Med. 54 (1988) 305–307, https://doi.org/10.1055/s-2006-962440.
[2] A. Yoshihisa, U. Takehito, F. Tsutomu, Novel acylated saponins from montbretia (*Crocosmia crocosmiiflora*): isolation of saponins and the structures of crocosmiosides A, B and H, Chem. Pharm. Bull. 37 (1989) 2139–2146, https://doi.org/10.1248/cpb.37.2139.
[3] A. Yoshihisa, U. Takehito, F. Tsutomu, Novel acylated saponins from montbretia (*Crocosmia crocosmiiflora*). II: the structures of crocosmiosides C, D, E, F, G and I, Chem. Pharm. Bull. 38 (1990) 142–149, https://doi.org/10.1248/cpb.38.142.
[4] S.C. Fry, The Growing Plant Cell Wall: Chemical and Metabolic Analysis, Reprint edition, The Blackburn Press, Caldwell, New Jersey, 2000 [ISBN 1-930665-08-3].
[5] H. Jork, W. Funk, W. Fischer, H. Wimmer, Thin-Layer Chromatography: Reagents and Detection Methods, vol. 1b, VCH, Weinheim, 1994.
[6] S. Perveen, A.M. Al-Taweel, S.Y. Hasan, A.F. Ghada, F. Ahmed, S.A. Maged, Hepatoprotective and cytotoxic activities of *Anvillea garcinii* and isolation of four new secondary metabolites, J. Nat. Med. 72 (2018) 106–117, https://doi.org/10.1007/s11418-017-1118-1.

[7] W. Ebrahim, M. El-Neketi, L.I. LewaldI, R.S. Orfali, W.H. Lin, N. Rehberg, R. Kalscheuer, G. Daletos, P. Proksch, Metabolites from the fungal endophyte *Aspergillus austroafricanus* in axenic culture and in fungal – bacterial mixed cultures, J. Nat. Prod. 79 (2016) 914–922, https://doi.org/10.1021/acs.jnatprod.5b00975.
[8] D.A.V. Berghe, A.J. Vlietinck, Screening methods for antibacterial and antiviral agents from higher plants, Methods Plant Biochem. 6 (1991) 47–68.
[9] A.R. El-Rokh, A. Negm, M. El-Shamy, M. El-Gindy, M. Abdel-Mogib, Sucrose diester of aryldihydronaphthalene-type lignans from *Echium angustifolium* Mill. and their antitumor activity, Phytochemistry 149 (2018) 155–160, https://doi.org/10.1016/j.phytochem.2018.02.014.
[10] Y.G. Gouda, A.M. Abdel-Baky, K.M. Mohamed, F.M. Darwish, R. Kasai, K. Yamasaki, Phenylpropanoid and phenylethanoid derivatives from *Kigelia pinnata* DC. Fruits, Nat. Prod. Res. 20 (2006) 935–939, https://doi.org/10.1080/14786410500462702.
[11] S.C. Fry, Cell wall polysaccharide composition and covalent crosslinking. Annual plant reviews, in: P. Ulvskov (Ed.), Vol. 41, Plant Polysaccharides, Biosynthesis and Bioengineering, Blackwell, 2011, pp. 1–42.
[12] C. Maier, J. Conrad, C.B. Steingass, U. Beifuss, R. Carle, R.M. Schweiggert, Quillajasides A and B: new phenylpropanoid sucrose esters from the inner bark of *Quillaja saponaria* Molina, J. Agric. Food Chem. 63 (2015) 8905–8911, https://doi.org/10.1021/acs.jafc.5b03532.
[13] A. Markovitz, Biosynthesis of guanosine diphosphate D-rhamnose + guanosine diphosphate D-talomethylose from guanosine diphosphate α-D-mannose, J. Biol. Chem. 239 (1964) 2091–2098 http://www.jbc.org/content/239/7/2091.
[14] V. Lanzotti, A. Romano, S. Lanzuise, G. Bonanomi, F. Scala, Antifungal saponins from bulbs of white onion, *Allium cepa* L, Phytochemistry 74 (2012) 133–139, https://doi.org/10.1016/j.phytochem.2011.11.008.
[15] H.M. Gao, Z.M. Wang, Triterpenoid saponins and phenylethanoid glycosides from stem of *Akebia trifoliata* var. *australis*, Phytochemistry 67 (2006) 2697–2705, https://doi.org/10.1016/j.phytochem.2006.09.003.
[16] D. Ramasamy, A. Saraswathy, Isolation of methyl 27-caffeoyloxyoleanolate—a new oleanane triterpenoid from the roots of *Hibiscus vitifolius*, Nat. Prod. Commun. 8 (2013) 433–434, https://doi.org/10.1177/1934578X1300800404.
[17] T. Rezanka, P. Rezanka, K. Sigler, Glycosides of arylnaphthalene lignans from *Acanthus mollis* having axial chirality, Phytochemistry 70 (2009) 1049–1054, https://doi.org/10.1016/j.phytochem.2009.05.016.